Catalytic Oxidation

DOI: 10.1002/anie.201406354

Oxidation of Bioethanol using Zeolite-Encapsulated Gold Nanoparticles**

*Jerrik Mielby, Jacob Oskar Abildstrøm, Feng Wang, Takeshi Kasama, Claudia Weidenthaler, and Søren Kegnæs**

Abstract: *With the ongoing developments in biomass conversion, the oxidation of bioethanol to acetaldehyde may become a favorable and green alternative to the preparation from ethylene. Here, a simple and effective method to encapsulate gold nanoparticles in zeolite silicalite-1 is reported and their high activity and selectivity for the catalytic gas-phase oxidation of ethanol are demonstrated. The zeolites are modified by a recrystallization process, which creates intraparticle voids and mesopores that facilitate the formation of small and disperse nanoparticles upon simple impregnation. The individual zeolite crystals comprise a broad range of mesopores and contain up to several hundred gold nanoparticles with a diameter of 2–3 nm that are distributed inside the zeolites rather than on the outer surface. The encapsulated nanoparticles have good stability and result in 50 % conversion of ethanol with 98 % selectivity toward acetaldehyde at 200 °C, which (under the given reaction conditions) corresponds to 606 mol acetaldehyde/mol Au hour^{-1}.*

As a consequence of the continuing depletion of fossil resources, the future chemical industry must gradually rely on renewable resources such as biomass to produce bulk and fine chemicals. Bioethanol, which is primarily used as fuel or fuel additive, is already produced from biomass and reached a production of 114 billion liters in 2013.[1,2] Crude bioethanol is produced by fermentation and contains up to 90 % water, which typically has to be removed before use.[3] The production of anhydrous bioethanol is an energy-demanding process, and it has therefore been suggested that bioethanol could be converted to value-added chemicals through reactions that are not sensitive to the water content.[4] For instance, bioethanol can be used as a renewable resource for the production of H_2 through catalytic steam reforming[5] or for the production of acetaldehyde,[6] acetic acid,[7] or ethyl acetate[8] through selective oxidation or dehydrogenation.[9,10] Currently, the main production of acetaldehyde is based on the oxidation of ethylene using a homogeneous catalytic system comprised of $PdCl_2$ and $CuCl_2$ (the Wacker process). As the cost of bioethanol is expected to decrease as a result of technological developments in biomass processing, it seems likely that converting bioethanol to acetaldehyde may become a favorable and green alternative to the ethylene route.

Since the first report on the high catalytic activity of supported gold nanoparticles in low-temperature CO oxidation,[11] they have been used for a number of reactions in organic chemistry. In particular, supported gold nanoparticles are highly active and selective catalysts for the aerobic oxidation of alcohols, including ethanol, in both liquid[4,7] and gas-phase.[12,13] Although the precise mechanistic details are still not fully understood, it is generally accepted that several factors contribute to the high catalytic activity of gold nanoparticles. In particular, they must typically be less than 10 nm in diameter, so that undercoordinated, reactive gold atoms exist in large numbers at the edges and corners of the particles.[14] However, as other metal catalysts, supported gold nanoparticles are prone to sintering, a thermal deactivation caused by Ostwald ripening or particle migration and coalescence.[15] The stability may be improved by tuning the catalyst composition and metal–support interactions[16] or by optimizing the three-dimensional distribution of the nanoparticles in ordered mesoporous materials.[17] Furthermore, highly stable catalysts have been obtained by encapsulation of individual nanoparticles in porous inorganic shells.[18] In 2010, Laursen et al.[19] reported the encapsulation of colloidal gold nanoparticles in zeolites during crystallization, and Li et al.[20] recently reported the synthesis of single gold nanoparticles in hollow zeolites prepared by recrystallization in tetrapropylammonium hydroxide (TPAOH). The researches demonstrated that the zeolite-encapsulated metal nanoparticles were extraordinarily size-selective[21] and remained active even after calcination at high temperatures. Although the encapsulation of single nanoparticles is an effective and elegant concept, bottom-up approaches often require complex procedures and expensive additives, which may prevent large-scale production.

Here, we report a simple and effective method to encapsulate gold nanoparticles in mesoporous silicalite-1 (Au/Recryst-S1) and demonstrate their high stability, catalytic activity, and selectivity for the gas-phase oxidation of bioethanol to acetaldehyde. The preparation of Au/Recryst-S1 was based on impregnation of recrystallized silicalite-1 prepared by an alkaline dissolution–reassembly

[*] J. Mielby, J. O. Abildstrøm, Prof. S. Kegnæs
Department of Chemistry, Technical University of Denmark
Kgs. Lyngby (Denmark)
E-mail: skk@kemi.dtu.dk
Dr. F. Wang, Dr. C. Weidenthaler
Max-Planck-Institut für Kohlenforschung
Mülheim an der Ruhr (Germany)
Dr. T. Kasama
Center for Electron Nanoscopy, Technical University of Denmark
Kgs. Lyngby (Denmark)

[**] The authors gratefully acknowledge the support of the Danish Council for Independent Research, Grant No. 2-127580.

Supporting information for this article is available on the WWW under http://dx.doi.org/10.1002/anie.201406354.

process in the presence of a surfactant. The alkaline dissolution was performed in an aqueous solution of ammonium hydroxide and cetyl trimethylammonium bromide (CTAB), and the reassembly was performed in an autoclave under hydrothermal conditions (see the Supporting Information). Based on the detailed mechanism recently reported by Ivanova et al.,[22,23] we propose that the alkaline dissolution breaks Si-O-Si bonds inside the zeolite, which causes the formation of intraparticle voids and mesopores. At this stage, the surfactant protects the zeolite from nonuniform leaching, which may result in the formation of large meso- and macropores.[24,25] Furthermore, the surfactant may diffuse into the zeolite, where it can form micelles and serve as template for the condensation of extracted siliceous species during the hydrothermal reassembly.[22] The recrystallized zeolite is calcined in air to remove the surfactant, dried under vacuum, and then impregnated with an aqueous solution of $HAuCl_4$, which fills up the voids and mesopores. As the material is dried and then reduced under H_2, the confined space of the zeolite framework provides ideal conditions for the preparation of small and disperse gold nanoparticles inside the zeolite crystals.[22,23]

Initially, the Au/Recryst-S1 catalyst was characterized by X-ray photoelectron spectroscopy (XPS). Compared to a conventional silicalite-1 catalyst with gold nanoparticles situated on the surface (Au/S1), we observed no signal at the Au $4f_{7/2}$ level for the recrystallized catalyst (Figure 1). As XPS is a surface-sensitive analysis, the absence of gold photopeaks indicated that the gold atoms were deposited inside the silicalite-1 crystals rather than on the outer surface.

Scanning transmission electron microscopy (STEM) provided more detailed information about the exact situation and size distribution of the gold nanoparticles. Electron tomography was performed by collecting STEM images at incremental degrees of rotation around the center of the zeolite crystal shown in Figure 1 A. Alignment and tomographic reconstruction of the collected images confirmed that the gold nanoparticles were situated inside the zeolite (see Figure 1 B, and Movie S1 in the Supporting Information). The gold nanoparticles were 2–3 nm in diameter and only a small fraction of the particles were situated on the surface of the zeolite. Furthermore, the tomographic reconstruction provided a unique insight into the voids and mesopores that were formed during the recrystallization process. Although there was no clear correlation between the distribution of nanoparticles and the internal mesopores, the observed porosity was in good agreement with the N_2 physisorption isotherm, which showed a typical H4 hysteresis loop that was nearly parallel at $P/P_0 > 0.45$ (Figure 2 A). It is noteworthy that the encapsulated gold nanoparticles were in principle too large to

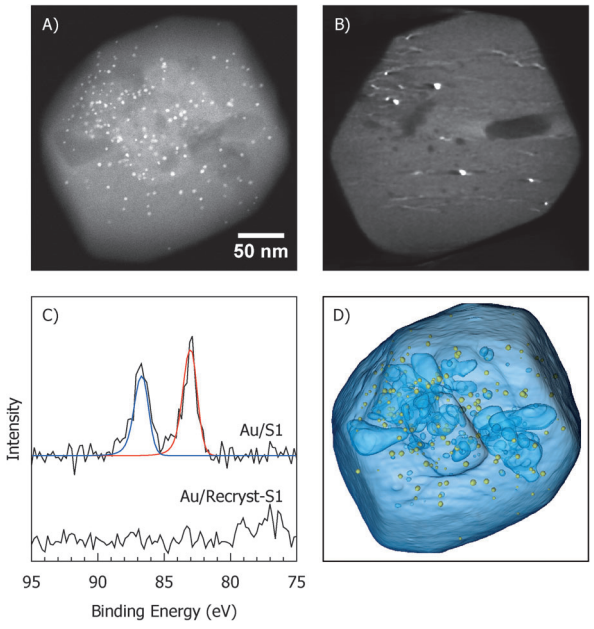

Figure 1. A) STEM image of Au/Recryst-S1. B) Reconstructed cross-section of Au/Recryst-S1. C) XPS spectrum of the Au 4f level of Au/S-1 and Au/Recryst-S1, respectively. D) 3D model of Au/Recryst-S1.

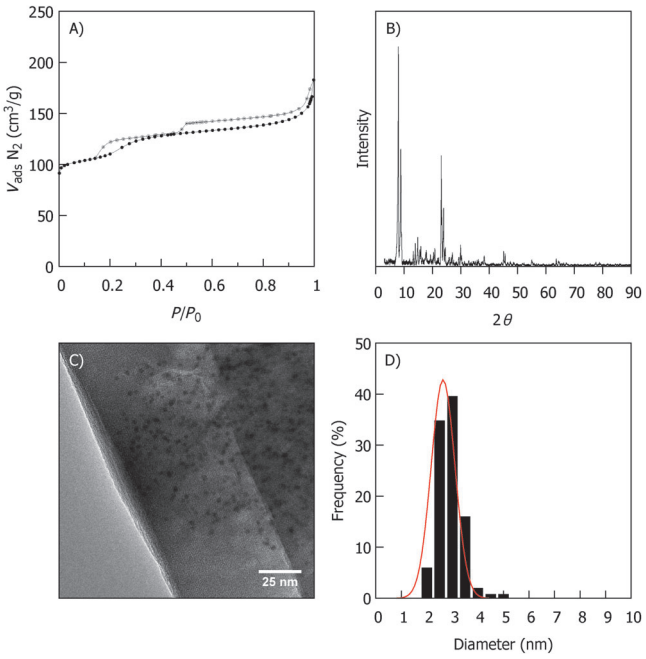

Figure 2. A) N_2 physisorption isotherm of Au/Recryst-S1 at 77 K. B) XRD pattern of Au/Recryst-S1 (MFI crystal structure). C) TEM image of Au/Recryst-S1. D) Size distribution based on measurements of approximately 250 nanoparticles by TEM.

fit into the micropores of silicalite-1. This indicated that the nanoparticles may be situated near small cracks or defects in the crystal structure. It is currently unclear if these imperfections were created during the recrystallization process or if the crystal structure was disrupted by the formation of gold nanoparticles upon reduction. Movies S2 and S3 show a 3D reconstruction of the Au/Recryst-S1 catalyst.

In order to investigate the effect of the zeolite support, the catalytic activity of Au/Recryst-S1 was compared to three other gold silicalite-1 catalysts. The first catalyst was prepared by impregnation of pure silicalite-1, followed by drying and reduction (Au/S1). The second catalyst was prepared by impregnation of a carbon-templated mesoporous silicalite-1 (Au/Meso-S1) following the method developed by Jacobsen

et al.[26] It has previously been demonstrated that carbon templating is an effective method to synthesize mesoporous zeolites and that the additional system of mesopores can increase the external surface area[27] and help to overcome diffusion limitations.[28,29] The third catalyst was prepared by impregnation of silicalite-1 modified with 3-aminopropyl trimethoxysilane (APS) in refluxing toluene (Au/APS-S1). The surface modification was performed in order to improve the gold–support interaction[30] and assist the formation of small and disperse nanoparticles. Detailed synthetic procedures and characterization by X-ray powder diffraction, XPS, TEM, and N_2 physisorption analysis can be found in the Supporting Information. An overview of the investigated catalysts is shown in Table 1

Table 1: Overview of the investigated catalysts.

Catalyst[a]	Diameter[b] [nm]	S_{ext}[c] [$m^2 g^{-1}$]	V_{micro}[c] [$cm^3 g^{-1}$]	V_{tot}[d] [$cm^3 g^{-1}$]	STY[e] at 200 °C
Au/S1	4.3 ± 1.7	65	0.116	0.192	44
Au/Meso-S1	3.3 ± 1.4	139	0.100	0.304	74
Au/APS-S1	2.4 ± 0.7	80	0.118	0.201	425
Au/Recryst-S1	2.6 ± 0.5	102	0.124	0.232	606

[a] Each catalysts was impregnated with 1 wt% Au. [b] Average diameter based on measurements of approximately 250 nanoparticles by TEM. [c] Calculated by the t-plot method. [d] Determined from the isotherm adsorption branch at around $P/P_0 = 0.95$. [e] Site–time yield (STY) in mol acetaldehyde/mol Au $hour^{-1}$.

In a typical experiment, an aqueous solution containing 10% ethanol was pumped into an evaporator together with He and atmospheric air corresponding to a molar ratio of O_2/ethanol = 1. The reactant gas was then passed through a fixed-bed reactor containing 100 mg fractionated catalyst. The reaction products were analyzed by an online GC-FID, while CO and CO_2 were analyzed by an online NDIR detector.

Figure 3 shows the product distribution as a function of the reaction temperature for the investigated catalysts. Each catalyst was impregnated with 1 wt% Au, which allowed a direct comparison of the catalytic activity. The Au/S1 catalyst was highly selective toward the formation of acetaldehyde and reached 50% conversion of ethanol at 280 °C. The Au/Meso-S1 catalyst was more active and reached 50% conversion at 250 °C. Only small amounts of CO_2 and acetic acid were observed at temperatures above 250 °C. The slightly higher activity of Au/Meso-S1 may be related to the increased external surface area, which results in a better dispersion of the Au nanoparticles.[27] The surface-functionalized Au/APS-S1 catalyst was more active than both Au/S1 and Au/Meso-S1, and reached 50% conversion of ethanol at 210 °C. At temperatures above 240 °C, however, the catalyst resulted in large amounts of acetic acid and CO_2, which significantly decreased the acetaldehyde yield. Au/Recryst-S1 was the most active catalyst and reached 50% conversion of ethanol with 98% selectivity toward acetaldehyde at 200 °C. Above 200 °C, the selectivity toward acetaldehyde started to decrease because of the formation of acetic acid. At 270 °C, both acetaldehyde and acetic acid were formed in 50% yield.

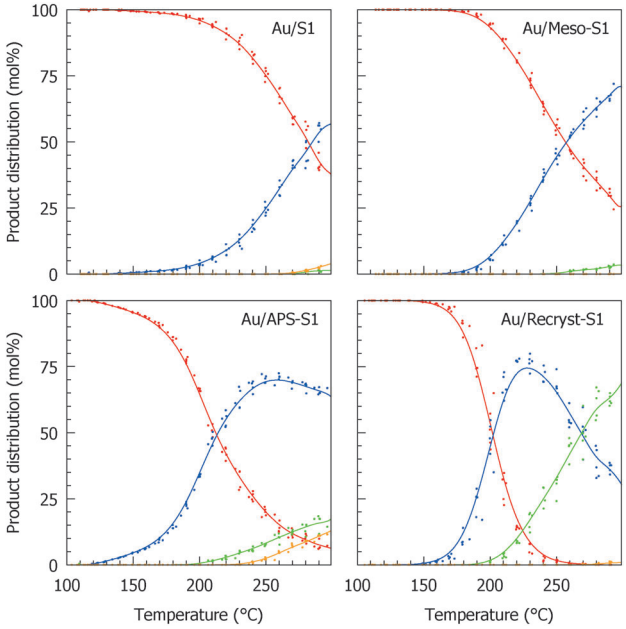

Figure 3. Product distribution of ethanol (red), acetaldehyde (blue), acetic acid (green), and CO_2 (orange) as function of the reaction temperature.

Surprisingly, no CO_2 was formed even at 300 °C. Since the size of the nanoparticles in Au/APS-S1 and Au/Recryst-S1 were almost the same, the results showed that the three-dimensional distribution of the nanoparticles had a significant effect on the activity. Compared to $Au/MgCuCr_2O_4$, which was recently reported to have a site–time yield (STY) as high as 1045 mol acetaldehyde/mol Au $hour^{-1}$ at 200 °C,[31] the corresponding STY of Au/Recryst-S1 was only 606, although it should be mentioned that the feed composition and space velocity were not directly comparable. The Au/Recryst-S1 catalyst showed good stability and even after 100 h of reaction at 200 °C, the Au/Recryst-S1 was still far more active than a commercial Au/TiO_2 catalyst, which resulted in an STY of 259 mol acetaldehyde/mol Au $hour^{-1}$ (see the Supporting Information).

SiO_2 has often been described as an inert support because it does not contribute to the supply and activation of oxygen as opposed to reducible metal oxides, such as TiO_2, CeO_2, or Fe_2O_3.[32] This does not mean that Au/SiO_2 (here in the form of silicalite-1) cannot be active, but that high catalytic activity requires very small Au nanoparticles with a high number of metal–support interfacial sites. It has previously been suggested that these sites may provide hydroxy groups that promote the reaction rate, presumable by participating in the reaction mechanism.[33,34] Our results demonstrate the importance of considering not only the size of the gold nanoparticles and the nature of the support material, but also the three-dimensional distribution and the structure of the gold–support interfacial sites.

In conclusion, we have developed a simple and effective method to encapsulate Au nanoparticles in recrystallized silicalite-1. The method is cost-effective, practical, and results in a narrow size distribution of small nanoparticles that are

situated inside the zeolite crystals, but remain readily accessible through the inherent microporous structure. The encapsulated nanoparticles were demonstrated to be highly active and selective for the catalytic gas-phase oxidation of ethanol to acetaldehyde. We therefore hope that impregnation of recrystallized zeolites will become a helpful tool in the development of many new nanostructured materials with unprecedented catalytic, magnetic, and optical properties.

Experimental Section

The detailed synthesis and characterization of all investigated catalysts by X-ray powder diffraction, XPS, TEM, and N_2 physisorption analysis is given in the Supporting Information.

Synthesis of 1 wt% Au/Recryst-S1: Tetraethyl orthosilicate (4.465 mL) was added dropwise to a tetrapropylammonium hydroxide solution (1.0 M, 7.265 mL) under stirring in a teflon beaker. The mixture was stirred for 1 hour and then heated in a teflon-lined stainless steel autoclave at 180 °C for 24 h under autogeneous pressure. The product was collected by filtration, washed with water, dried at room temperature, and then calcined for 20 h at 550 °C. The product silicalite-1 (1.0 g) was added to a solution of cetyl trimethylammonium bromide (0.7 g) in aqueous ammonium hydroxide (100 mL, 2.5 wt%) and stirred for 3 h at room temperature. The solution was then transferred to a teflon-lined stainless steel autoclave and heated to 140 °C for 24 h. The product was collected by filtration, washed with water, dried overnight, and then calcined at 550 °C for 5 h to remove the surfactant. The recrystallized silicalite-1 (0.9900 g) was predried in a vacuum oven at 50 °C and then impregnated with an aqueous solution of $HAuCl_4 \cdot 3H_2O$ (0.0199 g) to incipient wetness. The material was dried at room temperature overnight and then reduced in forming gas for 2 h at 350 °C to give the final gold catalyst.

Gas-phase oxidation of ethanol: An aqueous solution of 10% ethanol (0.05 mL min^{-1}) was pumped into an evaporator at 165 °C together with air (12.4 mL min^{-1}) and He (37.6 mL min^{-1}), which corresponded to a molar ratio of O_2/ethanol = 1. The preheated gas was then passed through a 3 mm stainless steel fixed-bed reactor containing 100 mg fractionated catalyst diluted with 100 mg of fractionated quartz (180–355 μm). The weight hourly space velocity was around 2.95 g ethanol/g catalyst h^{-1}. The product gas was periodically analyzed every 12 min by an online GC-FID equipped with a standard nonpolar column. All products were identified from gas samples by GC-MS and by the retention time of authentic samples on the online GC-FID. CO and CO_2 were detected by an online NDIR detector. All catalysts were tested under the same reaction conditions using a preprogrammed temperature profile from 110–300 °C increasing in 10 °C steps every hour to insure measurements at near steady-state conditions.

Received: June 18, 2014
Published online: September 1, 2014

Keywords: acetaldehyde · bioethanol · catalytic oxidation · gold nanoparticles · zeolite

[1] OECD-FAO Agricultural Outlook 2013, OECD Publishing **2013**, DOI: 10.1787/agr_outlook-2013-en.
[2] J. Goldemberg, *Science* **2007**, *315*, 808.
[3] S. Kumar, N. Singh, R. Prasad, *Renewable Sustainable Energy Rev.* **2010**, *14*, 1830.
[4] B. Jørgensen, s. E. Christiansen, M. L. D. Thomsen, C. H. Christensen, *J. Catal.* **2007**, *251*, 332.
[5] G. A. Deluga, J. R. Salge, L. D. Schmidt, E. E. Verykios, *Science* **2004**, *303*, 993.
[6] Y. Guan, E. J. M. Hensen, *J. Catal.* **2013**, *305*, 135.
[7] C. H. Christensen, B. Jørgensen, J. Rass-Hansen, K. Egeblad, R. Madsen, S. K. Klitgaard, S. M. Hansen, M. R. Hansen, H. C. Andersen, A. Riisager, *Angew. Chem. Int. Ed.* **2006**, *45*, 4648; *Angew. Chem.* **2006**, *118*, 4764.
[8] M. Nielsen, H. Junge, A. Kammer, M. Beller, *Angew. Chem. Int. Ed.* **2012**, *51*, 5711; *Angew. Chem.* **2012**, *124*, 5809.
[9] M. Murdoch, G. I. N. Waterhouse, M. A. Nadeem, J. B. Metson, M. A. Keane, R. F. Howe, J. Llorca, H. Idriss, *Nat. Chem.* **2011**, *3*, 489.
[10] T. Takei, N. Iguchi, M. Haruta, *Catal. Surv. Asia* **2011**, *15*, 80.
[11] M. Haruta, N. Yamada, T. Kobayashi, S. Iijima, *J. Catal.* **1989**, *115*, 301.
[12] A. Simakova, V. I. Sobolev, K. Y. Koltunov, B. Campo, A.-R. Leino, K. Kordás, D. Y. Murzin, *ChemCatChem* **2010**, *2*, 1535.
[13] V. I. Sobolev, K. Yu. Koltunov, O. A. Simakova, A.-R. Leino, D. Y. Murzin, *Appl. Catal. A* **2012**, *433*, 88.
[14] N. Lopez, T. V. W. Janssens, B. S. Clausen, Y. Xu, M. Mavrikakis, T. Bligaard, J. K. Nørskov, *J. Catal.* **2004**, *223*, 232.
[15] T. W. Hansen, A. T. DeLaRiva, S. R. Challa, A. K. Datya, *Acc. Chem. Res.* **2013**, *46*, 1720.
[16] J. A. Farmer, C. T. Campbell, *Science* **2010**, *329*, 933.
[17] G. Prieto, J. Zečević, H. Friedrich, K. P. de Jong, P. E. de Jong, *Nat. Mater.* **2013**, *12*, 34.
[18] P. M. Arnal, M. Comotti, F. Schüth, *Angew. Chem. Int. Ed.* **2006**, *45*, 8224; *Angew. Chem.* **2006**, *118*, 8404.
[19] A. B. Laursen, K. T. Højholt, L. F. Lundegaard, S. B. Simonsen, S. Helveg, F. Schüth, M. Paul, J.-D. Grunwalt, S. Kegnæs, C. H. Christensen, K. Egeblad, *Angew. Chem. Int. Ed.* **2010**, *49*, 3504; *Angew. Chem.* **2010**, *122*, 3582.
[20] S. Li, L. Burel, C. Aquino, A. Tuel, F. Morfin, J.-L. Rousset, D. Farrusseng, *Chem. Commun.* **2013**, *49*, 8507.
[21] S. Li, L. Burel, T. Boucheron, A. Tuel, D. Farrusseng, F. Meunier, *Chem. Commun.* **2014**, *50*, 1824.
[22] I. I. Ivanova, E. Knyazeva, *Chem. Soc. Rev.* **2013**, *42*, 3671.
[23] I. I. Ivanova, I. A. Kasyanov, A. A. Maerle, V. I. Zaikovskii, *Microporous Mesoporous Mater.* **2014**, *189*, 163.
[24] Y. P. Khitev, I. I. Ivanova, Y. G. Kolyagin, O. A. Ponomareva, *Appl. Catal.* **2012**, *441 – 442*, 124.
[25] V. V. Ordomsky, I. I. Ivanova, E. E. Knyazeva, V. V. Yuschenko, V. I. Zaikovskii, *J. Catal.* **2012**, *295*, 207.
[26] K. Johannsen, A. Boisen, M. Brorson, I. Schmidt, C. J. H. Jacobsen, *Stud. Surf. Sci. Catal.* **2002**, *142*, 109.
[27] C. H. Christensen, I. Schmidt, A. Carlsson, K. Johannsen, K. Herbst, *J. Am. Chem. Soc.* **2005**, *127*, 8098.
[28] I. Schmidt, A. Krogh, K. Wienberg, A. Carlsson, M. Brorson, C. J. H. Jacobsen, *Chem. Commun.* **2000**, 2157.
[29] J. Mielby, J. O. Abildstrøm, S. Pérez-Ferreras, S. B. Rasmussen, S. Kegnæs, *J. Porous Mater.* **2014**, DOI: 10.1007s10934-014-9800-0.
[30] L. M. Liz-Marzán, M. Giersig, P. Mulvaney, *Langmuir* **1996**, *12*, 4329.
[31] P. Liu, E. J. M. Hensen, *J. Am. Chem. Soc.* **2013**, *135*, 14032.
[32] M. M. Schubert, S. Hackenberg, A. C. van Veen, M. Muhler, V. Plzak, R. J. Behm, *J. Catal.* **2001**, *197*, 113.
[33] B. N. Zope, D. D. Hibbitts, M. Neurock, R. J. Davis, *Science* **2010**, *330*, 74.
[34] M. S. Ide, R. J. Davis, *Acc. Chem. Res.* **2014**, *47*, 825.

